




Facile preparation of magnetic sodium alginate/carboxymethyl cellulose composite hydrogel for removal of heavy metal ions from aqueous solution

Sisi Wu¹, Juan Guo¹, Ying Wang¹, Chao Huang^{1,*}, and Yong Hu^{1,*} 

¹ School of Food Science, Guangdong Pharmaceutical University, Zhongshan 528458, China

Received: 20 December 2020

Accepted: 24 March 2021

Published online:
13 April 2021

© The Author(s), under exclusive licence to Springer Science+Business Media, LLC, part of Springer Nature 2021

ABSTRACT

A novel magnetic polysaccharide composite hydrogel was successfully constructed by using sodium alginate (SA) and carboxymethyl cellulose (CMC) as the backbone and filled with in situ Fe₃O₄ nanoparticles, which was then employed for removal of heavy metal ion from aqueous solution. The obtained magnetic SA/CMC composite hydrogel was characterized by Fourier transform infrared spectroscopy, fluorescence microscope, thermogravimetric and vibrating sample magnetometer. Effect of contact time, pH and adsorbent dosage on the adsorption of heavy metal ions by the magnetic SA/CMC hydrogel have also been studied. The results show that the prepared magnetic SA/CMC hydrogel can be effectively utilized in the removal of heavy metal ions from aqueous solution. The maximal adsorption capacity of Mn(II), Pb(II), and Cu(II) as calculated from the Langmuir model were 71.83, 89.49, and 105.93 mg/g, respectively. The adsorption process of the magnetic SA/CMC hydrogel on the heavy metal ions can be attributed to ion exchange and chemical adsorption. What's more, the magnetic hydrogel exhibited high efficiency after four cycles, which indicating it offers great potential for practical application in the removal of heavy metal ions from aqueous solution.

Introduction

Pollution of aquatic ecosystems by heavy metals is one of the most important issues that has received special attention in recent years due to the rapid development of industry, agriculture, traffic, and

residential activities [1–3]. The discharge of heavy metal-containing wastewater into the environment can damage ecosystems and even threaten the health of humans through the food chain [4, 5]. Therefore, how to efficiently remove heavy metal ions has been a significant interest in research. It is particularly worth noting that heavy metals such as Mn(II), Pb(II),

Handling Editor: Maude Jimenez.

Address correspondence to E-mail: huangc@gdpu.edu.cn; lidhyong@126.com

and Cu(II) can be accumulated in the human body through inhalation, ingestion, drinking polluted water, and dermal contact, which may lead to potential damage to bone, brain, kidney, and liver [6–8]. In general, the methods for the removal of heavy metal ions from wastewater include electrolysis, reduction-precipitation, photocatalysis, membrane separation, ion exchange, and adsorption, etc. [9, 10]. Among these technologies, adsorption is regarded as one of the most promising ways for the removal of heavy metal ions due to inexpensive, superior efficiency, and nontoxic to the environment [11–14].

With the requirements for the recovery and reuse of specific heavy metals and the environmental demand, degradable adsorption materials such as sodium alginate (SA) and carboxymethyl cellulose (CMC) are increasingly used in the removal of heavy metal ion from wastewater due to the presence of various functional groups within them [15, 16]. SA is a natural polysaccharide extracted from brown algae. Due to the presence of free carboxyl groups and can be easily cross-linked by divalent and trivalent cations such as Ca^{2+} , Ba^{2+} , and Fe^{3+} to produce a stable gel, SA has been widely used in water treatment applications [17, 18]. In addition to SA, as an anionic polymeric obtained from the natural cellulose, CMC can also produce hydrogel by coordinating with multivalent cations such as Fe^{3+} and Al^{3+} , which make it possible for binding metal ions due to the presence of hydroxyl and carboxyl groups on the structure [19, 20].

Recently, it has been reported that nanomaterials such as magnetic nanoparticles, carbon nanotubes, graphene were used to compound with polysaccharide hydrogels to improve its adsorption and mechanical properties [21–23]. Among them, due to the simple preparation process, high specific surface area, and the ability to treat a large amount of wastewater in a short time without producing contaminants, the polysaccharide hydrogels incorporated with Fe_3O_4 magnetic nanoparticles have become the focus of adsorption research [24, 25]. However, although SA/CMC hydrogel has been investigated in some articles for the removal of heavy metal ions from aqueous solution, there is rare research on the preparation of magnetic SA/CMC composite hydrogel filled with in-situ formation of Fe_3O_4 nanoparticle by a green and facile method

without additional chemical cross-linking agents and organic solvents [26, 27].

In this work, the magnetic SA/CMC composite hydrogel filled with Fe_3O_4 nanoparticles was successfully constructed by co-precipitation and subsequent freezing–thawing method. A series of experiments were carried out to investigate the structural characteristics and adsorption performance of the magnetic SA/CMC composite hydrogel. The results demonstrate the magnetic composite hydrogel has good adsorption and solid–liquid separation performance, which can be used to remove heavy metal ions from contaminated aqueous solution.

Materials and methods

Materials

Sodium alginate (SA, viscosity, ≥ 200 mPa·s, average MW, 270 kDa) was purchased from Aladdin Chemistry Co., Ltd. Carboxymethyl cellulose (CMC, sodium salt, substitution degree $\geq 60\%$, average MW, 250 kDa) were purchased from Sinopharm Chemical Reagent Co., Ltd. Other reagents such as sodium hydroxide, ethanol, manganese nitrate, lead nitrate, copper sulfate, $\text{FeCl}_2 \cdot 4\text{H}_2\text{O}$, and $\text{FeCl}_3 \cdot 6\text{H}_2\text{O}$ were purchased from China National Pharmaceutical Corporation Limited. The chemical reagents were of analytical grade and employed directly without further purification. All solutions were prepared with distilled water.

Preparation of magnetic composite hydrogels

First, 2.50 g SA and 2.50 g CMC were weighed and dissolved in 100 ml deionized water under magnetic stirring at 600 rpm for 2 h to generate a homogeneous CMC/SA solution. Secondly, 6.41 g $\text{FeCl}_3 \cdot 6\text{H}_2\text{O}$ and 3.19 g $\text{FeCl}_2 \cdot 4\text{H}_2\text{O}$ were weighed and dissolved in 50 ml deionized water to form a uniform solution, and then was placed in CMC/SA solution followed by magnetic stirring for 1 h at room temperature. Finally, the dark brown color suspension solution after ultrasonic for 1 h was reduced by 0.1 mol/L ammonia until pH 9 and kept overnight at room temperature. The obtained gel was thoroughly rinsed with deionized water three times to remove

unreacted reagents, and then frozen and thawed three times to make the gel more uniformly cross-linked. Scheme 1 represents the formation of magnetic SA/CMC composite hydrogel. First, the compound solution of CMC and SA was cross-linked with Fe^{3+} and Fe^{2+} to form an inclusion complex, and then an appropriate amount of ammonia was added into the mixed iron-polysaccharide solution to form a magnetic composite hydrogel. Finally, the obtained magnetic composite hydrogel was subjected to freezing–thawing for further cross-linking.

Characterizations

The surface morphologies of the SA/CMC magnetic hydrogel were observed by fluorescence microscope (BX-50 Olympus, Japan). The functional groups of these samples were detected using Fourier transform infrared spectrophotometer (Nicolet 5700, American) by KBr pellet method in the range between 4000 and 500 cm^{-1} with a spectral resolution of 4 cm^{-1} and 20 scans. Thermogravimetric analysis (TGA) was measured under a nitrogen atmosphere with NetzschTG-209 from 40 to $600\text{ }^\circ\text{C}$ with a heating rate of $10\text{ }^\circ\text{C}/\text{min}$. Magnetization measurements were performed by Lakeshore 7400-S vibrating sample magnetometer (VSM).

Sorption experiments

In order to study the metal adsorption capacities of SA/CMC magnetic hydrogel, three types of heavy metal ions [Cu(II), Pb(II), and Mn(II)] were selected. The 0.01 g dry hydrogel was mixed in metal ion solutions, and then placed in a constant temperature vibrating shaker until the adsorption reaches equilibrium. At different intervals, the metal ion concentrations were determined by resonance light scattering (RLS) spectra, which were achieved by

means of a fluorescence spectrophotometer (RF5301-PC, Shimadzu, Japan) with $\Delta\lambda = 0\text{ nm}$. The pH values of the solution were adjusted by 0.1 M HCl or NaOH solutions. The adsorption rate (E), adsorption capacity (q_e), and distribution coefficient (K_d) were calculated according to the following equation:

$$E = \frac{C_0 - C_e}{C_0} \times 100\% \quad (1)$$

$$q_e = \frac{(C_0 - C_e)V}{m} \quad (2)$$

$$K_d = \frac{V(C_0 - C_e)C_e}{C_e \times m} \quad (3)$$

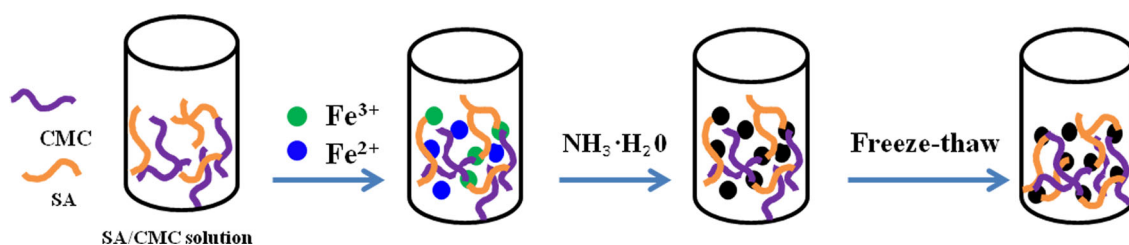
Here, C_0 (mg/L) and C_e (mg/L) are the initial concentrations of metal ions and the remaining metal ions concentration in the solution after adsorption equilibrium, respectively; V (L) represents the volume of the metal ions solution; m (g) indicates the weight of magnetic hydrogels.

Kinetics of adsorption

Crushed 0.01 g dry SA/CMC magnetic hydrogel sample was added to the 20 mL metal ion storage solution with an initial concentration of $100\text{ mg}\cdot\text{L}^{-1}$, and then was placed in a constant temperature vibrating shaker until the adsorption reaches equilibrium. The remaining metal ions concentration is analyzed to calculate the adsorption capacity. The kinetic rate of different metal ions adsorption on the magnetic hydrogels was investigated by using the pseudo-first-order, pseudo-second-order, and intra-particle diffusion models. The expressions are as follows:

$$\lg(q_e - q_t) = \lg q_e - k_1 t \quad (4)$$

$$\frac{t}{q_t} = \frac{1}{k_2 q_e^2} + \frac{t}{q_e} \quad (5)$$



Scheme 1 The scheme for constructing magnetic SA/CMC composite hydrogel.

$$q_t = k_{id}t^{1/2} + C \quad (6)$$

where q_e ($\text{mg}\cdot\text{g}^{-1}$) is the equilibrium adsorption capacity, q_t ($\text{mg}\cdot\text{g}^{-1}$) is the adsorption capacity in t time, k_1 (min^{-1}), k_2 ($\text{g}\cdot\text{mg}^{-1}\text{min}^{-1}$), and k_{id} ($\text{mg}\cdot\text{g}^{-1}\text{min}^{-0.5}$) are the rate constants of the pseudo-first-order, pseudo-second-order, and kinetic models, respectively. C is the boundary layer thickness.

Adsorption isotherm

The 0.01 g dry SA/CMC magnetic hydrogel was placed in a solution of 20 mL metal ions with initial concentrations of 10, 20, 40, 60, 100, 150, 200 $\text{mg}\cdot\text{L}^{-1}$, and then was shaken in a water bath oscillator for 24 h at room temperature. The remaining metal ions concentration was analyzed to calculate the adsorption capacity of the adsorbent. The adsorption isotherm was fitted by the Langmuir and Freundlich model equations. The expressions are as follows:

$$\frac{C_e}{q_e} = \frac{1}{K_L q_m} + \frac{C_e}{q_m} \quad (7)$$

$$\ln q_e = \ln K_F + \frac{1}{n} \ln C_e \quad (8)$$

In the formula, K_L and K_F are the constants related to adsorption in the Langmuir and Freundlich models, respectively; n is the Freundlich adsorption index, which is related to the properties of the adsorbent.

Competitive adsorption

Crushed 0.01 g dry SA/CMC magnetic hydrogel sample was added into a flask with 20 mL of a mixed solution containing three metal ions [Cu(II), Pb(II), and Mn(II)], and then was shaken in a thermostatic oscillator for 24 h at room temperature.

Desorption and regeneration

After the adsorption experiment is completed, the used magnetic hydrogel is eluted with 1 M HCl solution and regenerated with 0.1 M NaOH solution, and then washed with deionized water until it is neutral. According to the above method, the

regeneration performance was tested four times through the adsorption/desorption cycle, and each experiment used the same heavy metal ion solution.

Results and discussion

Characterization of SA/CMC magnetic hydrogel

The appearance and FM images of the SA/CMC magnetic hydrogel are displayed in Fig. 1. It can be observed from the surface of the magnetic hydrogel (Fig. 1a) that the hydrogel appeared to be rough and uneven. As seen from the FM image of freeze-dried magnetic hydrogel (Fig. 1b), the obtained magnetic hydrogel has a honeycomb porous network structure and can be considered suitable for the adsorption of metal ions.

The FTIR spectra of SA, CMC, and SA/CMC magnetic hydrogel were used to confirm the existence of the expected functional groups. As shown in Fig. 2b, c, both SA and CMC exhibit a common characteristic absorption peaks at about 3453 cm^{-1} , which can be attributed the stretching vibration of O–H. However, the stretching vibration peak of O–H in CMC/SA magnetic hydrogel is narrowed and moved to a low wavelength that is locked at 3418 cm^{-1} , indicating hydrogen bonds may occur between CMC and SA macromolecules [28]. The characteristic absorption peaks at 1622 cm^{-1} and 1413 cm^{-1} relating to the asymmetric and symmetric vibration of COO^- are occurred at 1618 cm^{-1} and 1396 cm^{-1} in a magnetic hydrogel, respectively, which indicating COO^- may participate in the cross-linking reaction. In addition, the characteristic peak belongs to the stretching vibration peak of C–O in pure SA and pure CMC is observed at 1028 cm^{-1} and 1030 cm^{-1} ,

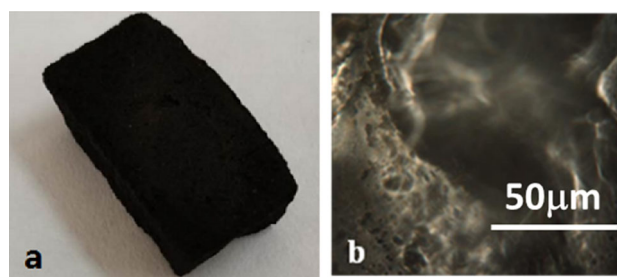


Figure 1 Appearance (a) and FM photographs (b) of magnetic SA/CMC hydrogel.

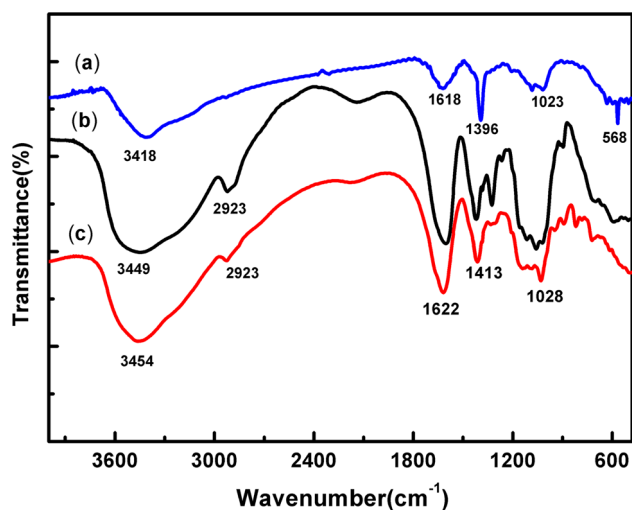


Figure 2 FTIR spectra of magnetic hydrogel (a), CMC (b) and SA (c).

respectively, while in CMC/SA magnetic hydrogel occurs at 1023 cm^{-1} . Other important consideration that the characteristic peak due to the stretching vibration of Fe–O is observed at 568 cm^{-1} , which demonstrates the presence of iron oxide in the hydrogel networks [29]. From the above analysis, it can be seen that the SA/CMC magnetic hydrogel has been generated successfully.

Thermogravimetric (TG) was carried out to examine the thermal stability of the SA/CMC magnetic hydrogel. As shown in Fig. 3a, the weight losses of SA are presented in two stages. The first stage appeared between 30 and $150\text{ }^{\circ}\text{C}$ due to the evaporation of moisture. The second stage appeared

between 250 and $300\text{ }^{\circ}\text{C}$ can be attributed to the breaking and losing of O–H groups on the alginate structure [30]. However, the TGA curve of SA/CMC magnetic hydrogel can be divided roughly into three stages. The first slight weight loss of 1.6% at $80\text{--}150\text{ }^{\circ}\text{C}$ due to the loss of adsorbed water in the sample. The other two weight loss step seen in the range of $250\text{--}350\text{ }^{\circ}\text{C}$ and $420\text{--}480\text{ }^{\circ}\text{C}$ can be ascribed to the network structural degradation of the magnetic hydrogel and the decomposition of molecular structure [31]. The different thermal degradation rates of the SA and CMC/SA magnetic hydrogel demonstrate the cross-linking reaction between chains, which leads to the formation of the composite adsorbent. The magnetization curve of SA/CMC magnetic hydrogel is shown in Fig. 3b. Obviously, the mild magnetic saturation value (3.2 emu g^{-1}) is attributed to the presence of Fe_3O_4 nanoparticles. The inset image further proves that the prepared hydrogel has good magnetic properties and can be used for the adsorption and separation of heavy metal ions.

Adsorption experiments

Resonance light scattering (RLS) is analytical technology that depends upon the measurements of light scattering of particles [32]. Particularly, when analytical conditions such as wavelength and pH are fixed, the RLS intensity is proportional only to the concentration of scattering particles [33]. It is shown in Fig. 4a, the RLS intensity of Cu(II) solution is very

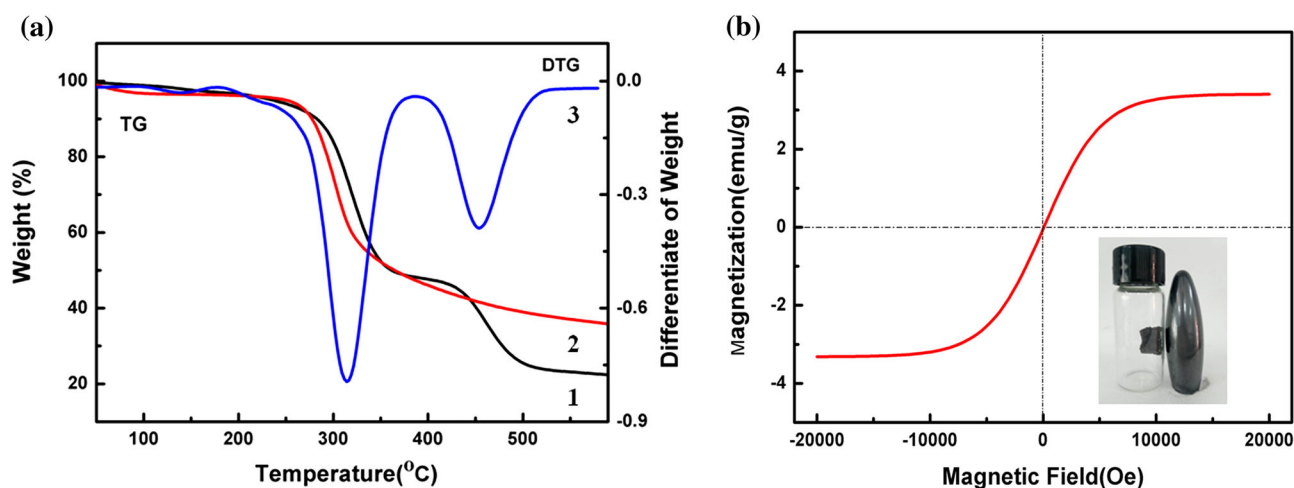


Figure 3 TGA of SA/CMC magnetic hydrogel (a1), SA(a2), and DTG of SA/CMC magnetic hydrogel (a3); Magnetization of SA/CMC magnetic hydrogel (b).

obvious. However, the RLS intensity of Cu(II) solution occurs remarkable decrease after the addition of CMC/SA magnetic hydrogel, which demonstrates that the absorption capacity of the magnetic hydrogel can be calculated by lowering the RLS intensity in solution. Figure 4b shows FTIR spectra of CMC/SA magnetic hydrogel before and after the adsorption of Cu(II) ions. After adsorbing Cu(II) ions, the asymmetric and symmetric vibration peak of COO^- at 1622 cm^{-1} and 1413 cm^{-1} are shifted to 1635 cm^{-1} and 1399 cm^{-1} , respectively, and the stretching vibration peak of C–O at 1023 cm^{-1} is almost disappeared. In view of the existence of electrostatic attraction and ion exchange reaction between $-\text{COO}^-$ and heavy metal ions in solution, it can be inferred that the COO^- group in magnetic hydrogel may play an important role in adsorption.

Since the prepared magnetic SA/CMC composite hydrogel can effectively adsorb copper ions, it is also considered to be able to adsorb other heavy metal ions such as lead and manganese ions. Figure 5a shows the effect of contact time on the adsorption of Cu(II), Mn(II), and Pb(II) by magnetic SA/CMC composite hydrogel. The observed order of absorption capacity of these metal ions to reach equilibrium is $\text{Cu(II)} > \text{Pb(II)} > \text{Mn(II)}$, which mainly related to the electronegativity and ionic radius of different heavy ions (the electronegativities for the Pb(II), Cu(II) and Mn(II) are 2.33, 1.90 and 1.55, respectively; the ionic radius for the Pb(II), Cu(II) and Mn(II) are 1.33 \AA , 0.72 \AA and 0.67 \AA , respectively). In addition, it can be seen that about 70% of total Mn(II), Cu(II),

and Pb(II) were absorbed by the magnetic hydrogel occurs within the first 50 min. The fast adsorption may be due to the three-dimensional loose and porous structure of the magnetic hydrogel, providing heavy metal ions with easier access to the adsorption sites. It also should be noted that there exist a slightly difference in contact time for each metal ion to reach the adsorption equilibrium, reflecting the differentiation of adsorption rate between different heavy metal ions and the magnetic SA/CMC hydrogel.

As is known to us, the initial pH of solution is another important parameter in the adsorption process of heavy metal ions [34]. Figure 5b shows the effect of solution pH on the adsorption of Pb(II), Cu(II), and Mn(II) by SA/CMC magnetic hydrogel. In the lower pH values (2.0–3.0), the adsorption capacity of the three heavy metal ions on the magnetic hydrogel starts to increase slowly may be due to part of the COO^- in the magnetic hydrogel combined with the H^+ in solution. As the pH value of the solution increases, the adsorption capacity for Pb(II) increases gradually in the pH range of 4–5, while for Cu(II) and Mn(II) in the range of 4–6. The reason is that the COO^- ions can fully combine with metal ions due to the decreasing amount of H^+ in solution, which leads to a remarkable increase in adsorption. However, further increasing the pH value of the solution shows different effects on the adsorption process. When the pH increases from 5.0 to 7.0, the adsorption amount of Pb(II) dropped rapidly, which can be due to and the precipitation in the form of Pb(OH)_2 [35]. For Cu(II), the adsorption capacity

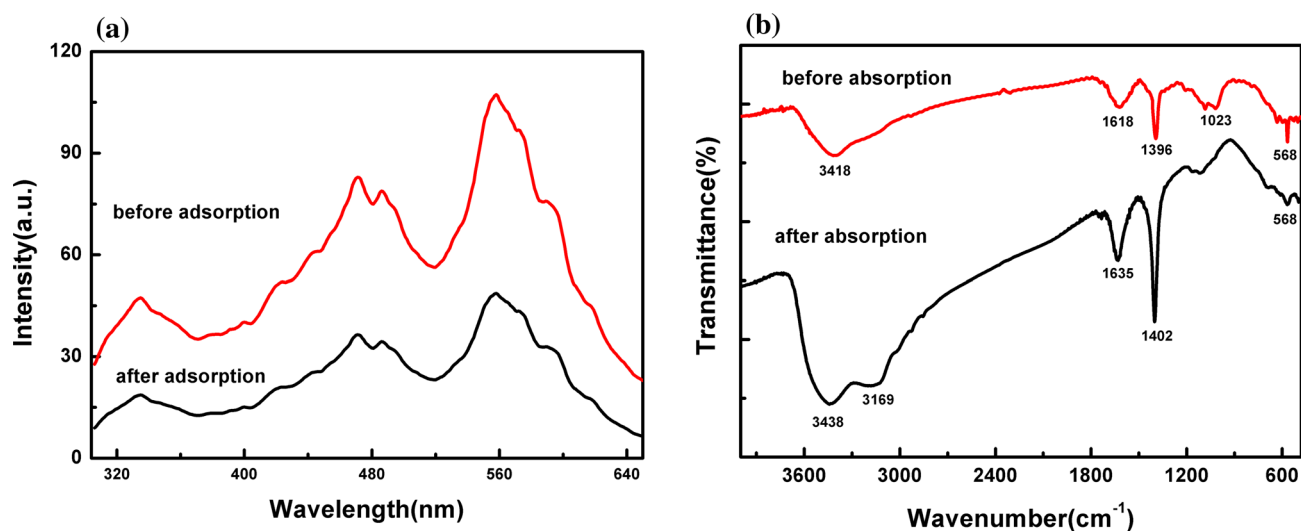


Figure 4 RLS (a) and FTIR (b) spectra of Cu^{2+} before and after treating with SA/CMC magnetic composite hydrogel.

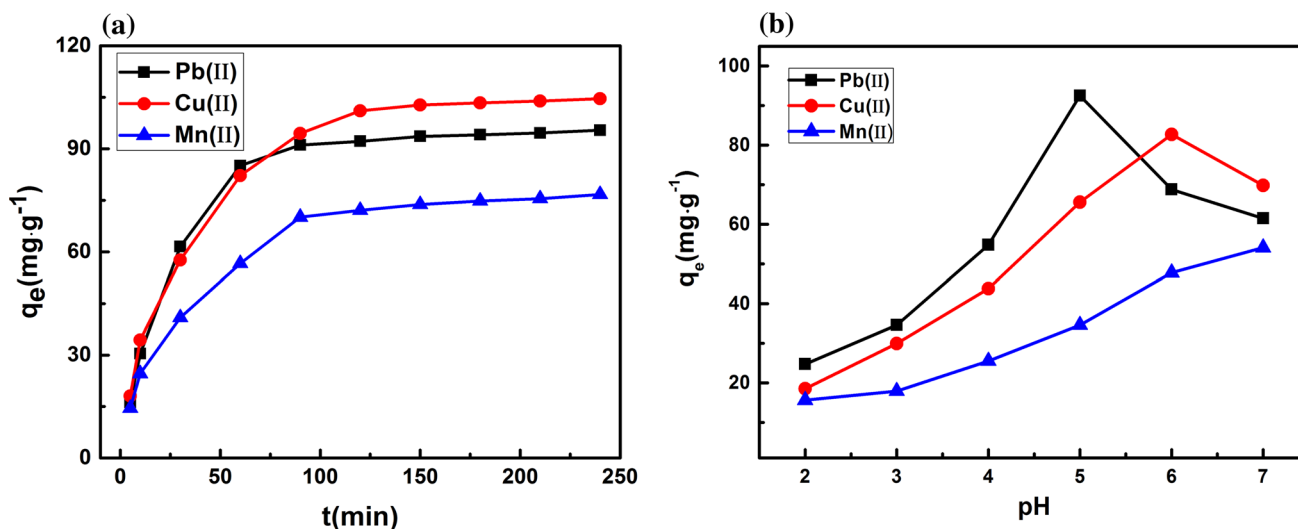


Figure 5 The effect of contact time (a) and pH (b) on adsorption capacity of SA/CMC magnetic hydrogel at room temperature.

begins to decrease when the pH is greater than 6. This can be attributed to OH^- ions react with metal ions at the active sites on the absorbent surface [36]. For Mn(II), the adsorption capacity continues to increase when the pH is greater than 6. This is because manganese usually precipitates at higher pH values than 8.0 [37].

Adsorption kinetics

The adsorption kinetics of three metal ions were investigated by using the pseudo-first-order, pseudo-second-order, and intraparticle diffusion models, and the results were depicted in Fig. 6. The calculated result of corresponding adsorption parameter values and correlation coefficients were presented in Table 1. It is found that the correlation coefficients of modeled pseudo-second-order by experiment data shown in Fig. 5a are larger than that of the pseudo-first-order and intraparticle diffusion model. Meanwhile, the equilibrium adsorption capacity calculated by the pseudo-second-order model is also closer to the experimental data. Therefore, the adsorption of metal ions by SA/CMC magnetic hydrogel can be better described by the pseudo-second-order kinetic model, which means the chemisorption dominates the adsorption of heavy metal ions [38]. In particular, an obvious inflection point can be found from the fitting results of the intra-particle diffusion model, which indicates that the adsorption of metal ions by the magnetic hydrogel may be divided into two stages [39]. The first linear stage ($t < 120$ min) is the

diffusion process of metal ions on the gel surface, and the second stage ($t > 120$ min) can be attributed to internal diffusion. Besides, although the fitting between q_t and $t^{1/2}$ exhibits a substantially linear relationship, the straight line does not pass through the origin, which demonstrates that the absorption of metal ions by the magnetic hydrogel is jointly controlled by multiple steps [40].

Adsorption isotherms

Isotherm is one of the important factors to understand the adsorption efficiency and explore the adsorption mechanism. Figure 7 shows the adsorption isotherms of Pb(II), Cu(II), and Mn(II) on SA/CMC magnetic hydrogel fitted by the Langmuir and Freundlich models, respectively. The corresponding parameters and correlation coefficients (R^2) are listed in Table 2. It can be seen from the fitting results in Table 2 that the adsorption process can be better explained by the Langmuir model, which suggests the adsorption process was carried out on the monolayer surface. Additionally, according to the value of n estimated by the Freundlich model, it can be inferred that there is a certain degree of heterogeneous adsorption between metal ions and magnetic hydrogel [41]. Therefore, the adsorption mechanism of metal ions by the SA/CMC magnetic hydrogel can be due to chemical adsorption accompanied ion exchange.

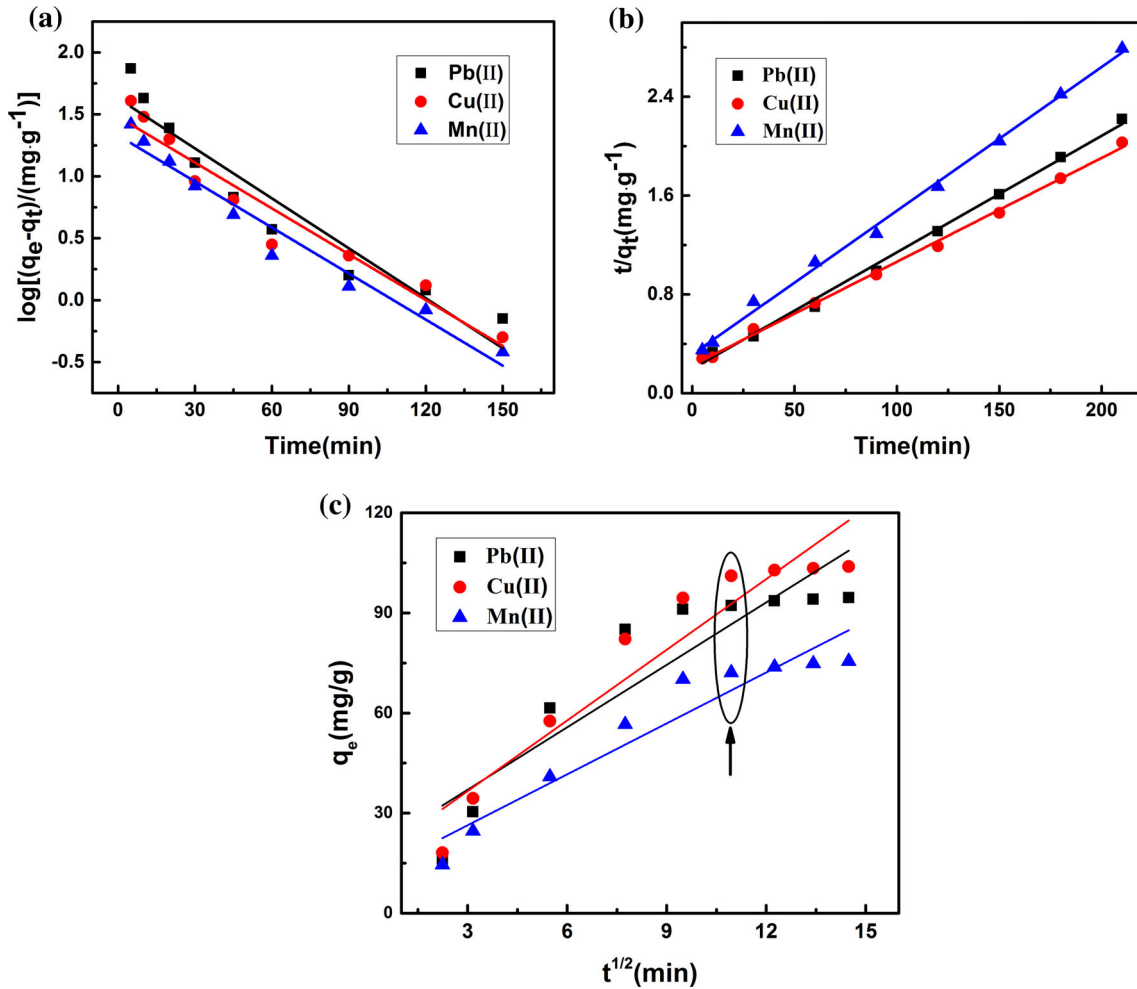


Figure 6 Pseudo-first-order (a), pseudo-second-order (b) and intraparticle diffusion (c) kinetic model on Cu (II), Pb (II) and Mn (II) ions adsorption.

Table 1 Kinetic parameter for metal ions adsorption on SA/CMC magnetic hydrogel

Metal ions	Q _{exp}	Pseudo-first-order			Pseudo-second-order			Intra-particle diffusion		
		q ₁	K ₁	R ²	q ₂	K ₂	R ²	K _{id}	C	R ²
Cu ²⁺	103.93	42.51	0.0134	0.906	108.91	0.0045	0.995	6.24	18.29	0.811
Pb ²⁺	93.76	30.13	0.0123	0.933	95.93	0.0032	0.997	7.06	15.39	0.895
Mn ²⁺	64.41	21.24	0.0124	0.959	65.91	0.0042	0.996	5.09	11.08	0.907

Competitive selective adsorption

The results of competitive selective adsorption of Cu(II), Pb(II), and Mn(II) are shown in Fig. 8. During the adsorption process, it can be seen that the amount of adsorption of Cu(II) by SA/CMC magnetic hydrogel is the largest, followed by Pb(II) and Mn(II). Additionally, the distribution coefficient of Cu(II) is the highest with the value of 64.03 L/g, while only 15.08 L/g for Mn(II), which further demonstrates the

competitive adsorption relationship between different metal ions and hydrogel. The main reason is that each metal ion has a different electronegativity and coordination ability with the SA/CMC magnetic hydrogel. Obviously, when the number of adsorption active sites of the adsorbing material is limited, the three metal ions will compete to adsorb the active sites in the material network.

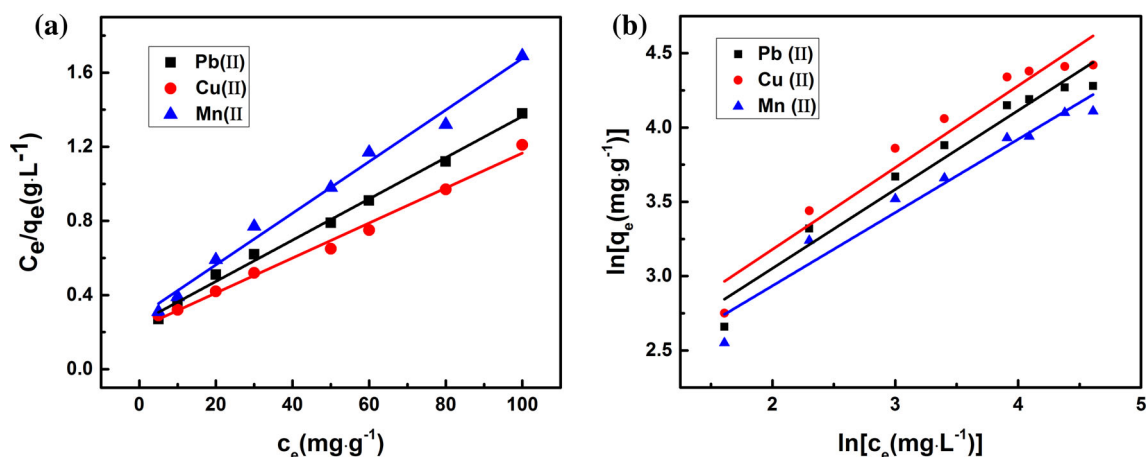


Figure 7 Langmuir (a) and Freundlich (b) isotherm model on Cu (II), Pb (II), Mn (II) ions adsorption.

Table 2 Langmuir and Freundlich parameters for adsorption on magnetic hydrogel

Metal ions	Q_{exp}	Langmuir coefficients			Freundlich coefficients		
		Q_{cai}	K_L	R^2	K_f	n	R^2
Cu^{2+}	103.93	105.93	0.0424	0.990	8.81	1.882	0.951
Pb^{2+}	93.76	89.49	0.0443	0.994	7.31	1.816	0.933
Mn^{2+}	64.41	71.83	0.0489	0.987	5.05	2.027	0.948

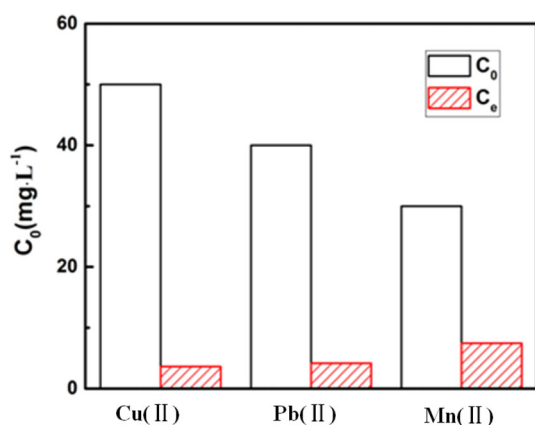


Figure 8 Selective adsorption of the SA/CMC magnetic hydrogel.

Adsorbent recycling

The results of recovery efficiency of metal ions by SA/CMC magnetic hydrogel are shown in Fig. 9. As it indicated, the adsorption efficiency of the three metal ions is gradually decreased after adsorption/stripping cycles. In the first cycle, the removal efficiency is 92.1%, 90.1%, and 79.9% for Cu(II), Pb(II), and Mn(II), respectively. At the end of the fourth cycle, the adsorption efficiency of Cu(II), Pb(II), and Mn(II) can reach 65.3%, 61.7%, and 58.6%,

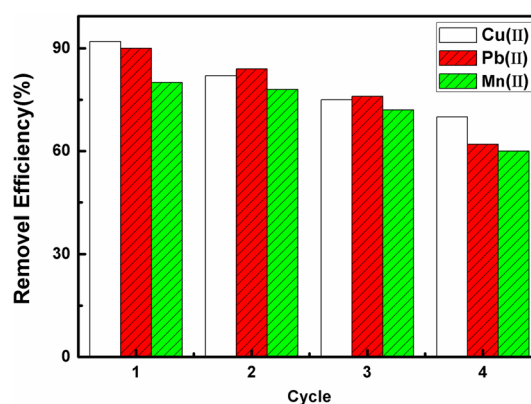


Figure 9 Removal efficiency after adsorption–desorption cycles.

respectively. The results show that, although part of the functional groups was destroyed after acid treatment, the magnetic hydrogel still retains a better desorption cycle utilization rate.

Conclusion

In this study, the magnetic SA/CMC hydrogel was prepared with a simple and green preparation approach, and its adsorption of Cu(II), Pb(II), and Mn(II) was studied experimentally. Results showed

that the adsorption equilibrium was substantially reached in about 240 min and the adsorption capacity for Cu(II), Pb(II), and Mn(II) were 105.93, 89.49, and 71.83 mg/g, respectively. Additionally, the adsorption kinetics could be better described by pseudo-second-order and the adsorption isotherms were fitted better with the Langmuir model. It was also examined that the magnetic SA/CMC hydrogel had good removal efficiency after four circulations. It is expected that the magnetic composite hydrogel will potentially be used to remove heavy metal contaminants from aquatic systems.

Acknowledgements

This work was financially supported by the Science and Technology Program of Zhongshan (Grant No. 2020B2068, 2020B2005) and Natural Science Foundation of Guangdong Province (Grant No. 2018A030310477, 2019A1515011843)

Author contributions

Hu Yong: Conceptualization, Methodology, Writing-original draft, Funding acquisition. Wu Sisi: Experiment investigation, Data curation. Guo Juan: Instrumental analysis, Funding acquisition. Wang Ying: Instrumental analysis. Huang Chao: Writing- review.

Declarations

Conflict of interest The authors declare that they have no known competing financial interests or personal relationships that could have appeared to influence the work reported in this paper.

References

- [1] Jaiswal A, Verma A, Jaiswal P (2018) Detrimental effects of heavy metals in soil, plants, aquatic ecosystem as well as in humans. *J Environ Pathol Toxicol Oncol* 37:183–197
- [2] Ebqa'ai M, Ibrahim B (2017) Application of multivariate statistical analysis in the pollution and health risk of traffic-related heavy metals. *Environ Geochem Health* 39:1441–1456
- [3] Song Q, Li J (2014) Environmental effects of heavy metals derived from the waste recycling activities in China: a systematic review. *Waste Manage* 34:2587–2594
- [4] Li Z, Ma T, Yuan C, Hou JY, Wang QL, Wu LH, Christie P, Luo YM (2016) Metal contamination status of the soil-plant system and effects on the soil microbial community near a rare metal recycling smelter. *Environ Sci Pollut Res* 23:17625–17634
- [5] Zhao Y, Xu M, Liu Q, Wang Z, Zhao L, Chen Y (2018) Study of heavy metal pollution, ecological risk and source apportionment in the surface water and sediments of the jiangsu coastal region, china: a case study of the sheyang estuary. *Mar Pollut Bull* 137:601–609
- [6] Ibrahim F, Nomier MA, Sabik LME, Shaheen MA (2020) Manganese-induced neurotoxicity and the potential protective effects of lipoic acid and spirulina platensis. *Toxicol Mech Method* 30:497–507
- [7] Kumar MR, Reddy KS, Reddy AG, Reddy RA, Reddy DG (2011) Lead-induced hepatotoxicity and evaluation of certain antistress adaptogens in poultry. *Toxicol Int* 18:62–66
- [8] Letelier ME, Lepe AM, Faúndez M, Salazar J, Marín R, Aracena P, Speisky H (2005) Possible mechanisms underlying copper-induced damage in biological membranes leading to cellular toxicity. *Chem-Biol Interact* 151:71–82
- [9] Fu FL, Wang Q (2011) Removal of heavy metal ions from wastewaters: a review. *J Environ Manage* 92:407–418
- [10] Zhu Y, Fan WH, Zhou TT, Li XM (2019) Removal of chelated heavy metals from aqueous solution: a review of current methods and mechanisms. *Sci Total Environ* 678:253–266
- [11] Xiang T, Zhang ZL, Liu HQ, Yin ZZ, Li L (2013) Liu XM (2013) Characterization of cellulose-based electrospun nanofiber membrane and its adsorptive behaviour using Cu(II), Cd(II), Pb(II) as models. *Sci China Chem* 56:567–575
- [12] Hussain MS, Musharraf SG, Bhangar MI, Malik MI (2020) Salicylaldehyde derivative of nano-chitosan as an efficient adsorbent for lead(II), copper(II), and cadmium(II) ions. *Int J Biol Macromol* 147:643–652
- [13] Godiya CB, Cheng X, Li DW, Chen Z, Lu XL (2019) Carboxymethyl cellulose/polyacrylamide composite hydrogel for cascaded treatment/reuse of heavy metal ions in waste water. *J Hazard Mater* 364:28–38
- [14] Hu Y, Wu XY, He X, Xing D (2019) Phosphorylated polyacrylonitrile-based electrospun nanofibers for removal of heavy metal ions from aqueous solution. *Polym Adv Technol* 30:545–551
- [15] Kim MS, Park SJ, Gu BK, Kim CH (2012) Ionically crosslinked alginate carboxymethyl cellulose beads for the delivery of protein therapeutics. *Appl Surf Sci* 262:28–33
- [16] Hu ZH, Omer AM, Ouyang XK, Yu D (2018) Fabrication of carboxylated cellulose nanocrystal/sodium alginate hydrogel

- beads for adsorption of Pb(II) from aqueous solution. *Int J Biol Macromol* 108:149–157
- [17] Anamizu M, Tabata Y (2019) Design of injectable hydrogels of gelatin and alginate with ferric ions for cell transplantation. *Acta biomater* 100:184–190
- [18] Edathil AA, Alhseina E, Banat F (2019) Removal of heat stable salts from industrial lean methyldiethanolamine using magnetic alginate/iron oxide hydrogel composite. *Int J Greenh Gas Con* 83:117–127
- [19] Swamy BY, Yun YS (2015) In vitro release of metformin from iron (III) cross-linked alginate-carboxymethyl cellulose hydrogel beads. *Int J Biol Macromol* 77:114–119
- [20] Ure D, Mutus B (2021) The removal of inorganic phosphate from water using carboxymethyl cellulose-iron hydrogel beads. *J chem Technol Biot* 96:38–47
- [21] Nagireddy NR, Yallapu MM, Kokkarachedu V, Sakey R, Kanikireddy V, Alias JP, Konduru MR (2011) Preparation and characterization of magnetic nanoparticles embedded in hydrogels for protein purification and metal extraction. *J Polym Res* 18:2285–2294
- [22] Zhu HY, Fu YQ, Jiang R, Yao J, Xiao L, Zeng GM (2012) Novel magnetic chitosan/poly(vinyl alcohol) hydrogel beads: preparation, characterization and application for adsorption of dye from aqueous solution. *Bioresource Technol* 105:24–30
- [23] Wang WB, Zhang HX, Shen JF, Ye MX (2018) Facile preparation of magnetic chitosan/poly (vinyl alcohol) hydrogel beads with excellent adsorption ability via freezing-tawing method. *Colloid Surface A* 553:672–680
- [24] Facchia DP, Cazettac AL, Canesina EA, Almeida VC, Bonafêa EG, Kipperd MJ, Martins AF (2018) New magnetic chitosan/alginate/Fe₃O₄@SiO₂ hydrogel composites applied for removal of Pb(II) ions from aqueous systems. *Chem Eng J* 337:595–608
- [25] Zhang H, Omer AM, Hu ZH, Yang LY, Ji C, Ouyang XK (2019) Fabrication of magnetic entonite/carboxymethyl chitosan/sodium alginate hydrogel beads for Cu (II) adsorption. *Int J Biol Macromol* 135:490–500
- [26] Zhang YP, Li ZK (2017) Heavy metals removal using hydrogel-supported nanosized hydrous ferric oxide: synthesis, characterization, and mechanism. *Sci. Total Environ.* 580:776–786
- [27] Zhang SY, Gao H, Guo PT, Li TL, Lin TS, Ding R, Wang ZB, He P (2020) Fabrication and extrusion of the PAAm SAAlg hydrogels with magnetic particles. *Colloid Surface A* 603:125280
- [28] Ren HX, Gao ZM, Wu DJ, Jiang JH, Sun YM, Luo CW (2016) Efficient Pb(II) removal using sodium alginate-carboxymethyl cellulose gel beads: preparation, characterization, and adsorption mechanism. *Carbohydr Polym* 137:402–409
- [29] Hu XY, Wang YM, Zhang LL, Xu M, Zhang JF, Dong W (2018) Design of a pH sensitive magnetic composite hydrogel based on salectan graft copolymer and Fe₃O₄@SiO₂ nanoparticles as drug carrier. *Int J Biol Macromol* 107:1811–1820
- [30] Jeddi MK, Mahkam M (2019) Magnetic nano carboxymethyl cellulose-alginate /chitosan hydrogel beads as biodegradable devices for controlled drug delivery. *Int J Biol Macromol* 135:829–838
- [31] Dai HJ, Zhang H, Ma L, Zhou HY, Yu Y, Guo T, Zhang YH, Huang HH (2019) Green pH/magnetic sensitive hydrogels based on pineapple peel cellulose and polyvinyl alcohol: synthesis, characterization and naringin prolonged release. *Carbohydr Polym* 209:51–61
- [32] Kaewprom C, Nuengmatcha P, Chanthai S (2018) Diethyldithiocarbamate doped graphene quantum dots based metal complex nanoparticles by resonance light scattering for green detection of lead(II). *Oriental J Chem* 34:623–630
- [33] Hu Y, Fu X, Chen XD, Zhong NJ (2012) Solution properties of mixed starch/chitosan revealed by resonance light scattering. *Chem Res Chin Univ* 28:1107–1111
- [34] Li J, Tong JJ, Li XH, Yang ZJ, Zhang YC, Diao GW (2016) Facile microfluidic synthesis of copolymer hydrogelbeads for the removal of heavy metal ions. *J Mater Sci* 51:10375–10385. <https://doi.org/10.1007/s10853-016-0258-0>
- [35] Kosa SA, Al-Zhrani G, Salam MA (2012) Removal of heavy metals from aqueous solutions by multi-walled carbon nanotubes modified with 8-hydroxyquinoline. *Chem Eng J* 182:159–168
- [36] Maity J, Ray SK (2017) Competitive removal of Cu(II) and Cd(II) from water using a biocomposite hydrogel. *J Phys Chem B* 121:10988–11001
- [37] Lee SM, Tiwari D, Choi KM, Yang JK, Chang YY, Lee HD (2009) Removal of Mn(II) from aqueous solutions using manganese-coated sand samples. *J Chem Eng Data* 54:1823–1828
- [38] Li Z, Chen J, Ge Y (2017) Removal of lead ion and oil droplet from aqueous solution by lignin-grafted carbon nanotubes. *Chem Eng J* 308:809–817
- [39] Jiang HB, Yang YR, Lin ZK, Zhao BC, Wang J, Xie J, Zhang AP (2020) Preparation of a novel bio-adsorbent of sodium alginate grafted polyacrylamide graphene oxide hydrogel for the adsorption of heavy metal ion. *Sci Total Environ* 744:140653
- [40] Zhao BC, Jiang HB, Lin ZK, Xu SF, Xie J, Zhang AP (2019) Preparation of acrylamide/acrylic acid cellulose hydrogels

for the adsorption of heavy metal ions. Carbohydr Polym 224:115022

- [41] Mao SM, Liu XJ, Alharbi NS, Rohani S, Lu J (2018) Fabrication of xanthate-modified chitosan/poly(N-sopropylacrylamide) composite hydrogel for the selective adsorption

of Cu(II), Pb(II) and Ni(II) metal ions. Chem Eng Res Des 39:197–210

Publisher's Note Springer Nature remains neutral with regard to jurisdictional claims in published maps and institutional affiliations.